Impact of chemically defined media conditions on the production and regenerative function of mesenchymal stem cell-derived extracellular vesicles

The more the merrier

Eva Sievers
5415039
Science and Business Management
Major Research Project (51 EC)

UMC Utrecht - Department of Experimental Cardiology
Supervisors: Dr. Pieter Vader and Christian Snijders Blok
Second examiner: Dr. Raymond Schiffelers

Universiteit Utrecht

UMC Utrecht

List of abbreviations

APC	Allophycocyanin
AT	Adipose tissue
BCA	Bicinchoninic acid
BM	Bone marrow
BSA	Bovine serum albumin
CDM-HD	Chemically defined medium for high density cell culture
CVD	Cardiovascular disease
EV	Extracellular vesicle
FBS	Fetal bovine serum
FITC	Fluorescein isothiocyanate
HF	Heart failure
HfMSC	Human fetal mesenchymal stem cell
HfMSC-EV	Human fetal mesenchymal stem cell-derived extracellular vesicle
HMEC-1	Human microvascular epithelial cell-1
I/R	Ischemia/reperfusion
ISCT	International Society for Cell and Gene Therapy
LDS	Lithium dodecyl sulphate
M+CDM	MEM-α containing 10% chemically defined medium for high density cell culture
MSC	Mesenchymal stem cell
MSC-EV	Mesenchymal stem cell-derived extracellular vesicle
NTA	Nanoparticle tracking analysis
OM+CDM	Opti-MEM containing 10% chemically defined medium for high density cell culture
P/S	Penicillin/streptomycin
PBS	Phosphate-buffered saline
PC	Procedural control
PP	Polypropylene
PVDF	Polyvinylidene difluoride
RIPA	Radioimmunoprecipitation assay
RT	Room temperature
SD	Standard deviation
SEC	Size-exclusion chromatography
TBS	Tris-buffered saline
TBS-T	Tris-buffered saline containing 0.1% Tween-20
UC	Ultracentrifugation

Abstract

The use of mesenchymal stem cell-derived extracellular vesicles (MSC-EVs) have gained much attention because of their therapeutic potential for cardiac repair. However, their translation to the clinic is dependent on overcoming challenges, such as large-scale extracellular vesicle (EV) production. Although serum starvation is a widely used technique to increase EV production, it remains insufficient for large-scale production. On that note, a chemically defined medium for high density cell culture (CDM-HD) is believed to increase MSC-EV production in hollow fiber bioreactors; however, no comparative analysis has been performed between EVs from CDM-HD-cultured MSCs and starved MSCs in 2D cell culture systems. Therefore, this project aimed to assess the effects of culture conditions with CDM-HD on the production of human fetal MSC-EVs, and whether these EVs are functional. For the comparative analysis, EV yields from MSCs cultured in Opti-MEM or MEM-α with 10% CDM-HD supplementation or without (starvation) were determined using nanoparticle tracking analysis and western blot analysis. EV functionality was assessed using a scratch wound assay. The results showed that when compared to their starvation counterpart, Opti-MEM with CDM-HD (OM+CDM) resulted in the highest EV yield with a 9.6-fold increase within 24h, whereas within 48h, MEM-α with CDM-HD (M+CDM) increased EV yield with 17.2-fold. Regarding EV functionality, M+CDM EVs were able to induce endothelial cell migration; however, minor differences were observed with the procedural control. Taken together, culturing with CDM-HD increases EV yield to a greater extent than serum starvation. However, M+CDM EV functionality should be further explored to realize its potential as therapeutic agent for cardiac repair.

Layman summary

To date, there is an increasing need for suitable therapies to treat cardiovascular diseases, especially heart failure (HF). HF is a long-term condition in which the heart muscle is damaged, resulting in the inability to efficiently pump blood throughout the body. Standard treatments for HF comprise of methods that focus on easing the symptoms, whereas they fail to repair the damaged heart muscle. Therefore, alternatives to these treatments should be explored. In particular, mesenchymal stem cells (MSCs) release membrane particles, named extracellular vesicles (EVs), that contain information that among other things, aids in the repair of cells. However, their application as a therapy is complicated since cells do not produce enough EVs for medicinal purposes. Specific changes in the growth conditions of cells, such as serum deprivation, are known to increase EV production by causing cellular stress. Although these changes remain insufficient to meet large-scale requirements, cellular stress has also been shown to alter the properties of cells and their EVs.

Therefore, growth medium substitutes, such as FiberCell Systems' chemically defined medium for high-density cell culture (CDM-HD), are being developed to minimize cellular stress while increasing EV production. However, the effect of CDM-HD on the EV production from MSCs in static cell growth systems and whether these EVs possess healing abilities has not been extensively studied. Therefore, this project aimed to uncover the effects of CDM-HD dissolved in growth medium, Opti-MEM (OM+CDM) or MEM-α (M+CDM), on cell liveliness, cell shape, and EV production, and to compare this to serum-deprived human fetal MSCs and their EVs after 24 and 48h of incubation.

It was found that when the cells were grown with CDM-HD for 24 and 48h, liveliness was unaffected and the cells maintained their shape. Furthermore, OM+CDM resulted in the highest EV production after 24h, whereas M+CDM led to the highest increase after 48h. Similarly, an increase in EV protein expression was found for both CDM-HD samples. These data demonstrate that CDM-HD enables efficient and robust production of EV quantities in static cell growth systems and shows potential for large-scale manufacturing. Furthermore, the wound healing ability of EVs from M+CDM was investigated in a scratch wound experiment. The M+CDM EVs were found to be able to stimulate wound closure; however, minor differences with the negative control were observed. Therefore, it is recommended that in future studies the determination of optimal EV dosage and a better understanding of the influence of EV sample preparations and cell source are needed to uncover their full potential as EV-based therapies to treat HF.

Introduction

Cardiovascular disease (CVD) is the leading cause of mortality worldwide, of which heart failure (HF) is one of the primary causes of morbidity. HF is a chronic condition caused by structural or functional abnormalities in the myocardium, that results in the incapability to maintain an adequate cardiac output that meets the metabolic requirements of the human body. These abnormalities are characterized by the severe loss of cardiomyocytes and are often the result of cardiac injury due to a myocardial infarction[1]. In terms of HF survival rates, a study combining the Framingham Heart Study and Cardiovascular Health Study cohorts found an approximate 55% mortality rate within 5 years after diagnosis[2]. Furthermore, for those that are refractory to conventional drug therapy, a complete heart transplantation remains the gold standard. However, with the current organ donor shortages, these demands can simply not be met[1]. Therefore, alternatives to conventional therapies should be explored.

For instance, the use of mesenchymal stem cells (MSCs) as therapeutic agents to stimulate cardiac regeneration has gained much attention within the field of regenerative medicine[3]. MSCs are multipotent, non-hematopoietic cells that can be isolated from a variety of sources, including adipose tissue (AT) and bone marrow (BM)[4]. Initially, the therapeutic efficacy of MSCs was thought to be achieved directly through differentiation to replace the damaged cells[5]. However, MSC-based therapies have yet to demonstrate clinically significant improvements in outcomes due to limitations, such as inadequate cell survival rates and poor engraftment in the infarcted region[6,7]. Moreover, it became apparent that the therapeutic effects of MSCs are predominantly mediated by their secretion of paracrine factors, particularly their derived extracellular vesicles (EVs)[5].

EVs are nano-sized membrane-enclosed particles that are secreted by cells and mediate intercellular communication by the transfer of their bioactive cargo and through activation via receptor-ligand interactions[8,9]. Generally, EVs can be divided into three main populations based on their size and biogenesis: exosomes, microvesicles, and apoptotic bodies[9]. Exosomes (40–100 nm) are generated through the endocytic pathway and are released via exocytosis, whereas microvesicles (40–1000 nm) are formed by the outward budding and fission of the plasma membrane, and apoptotic bodies (1000–5000 nm) are formed due to membrane blebbing during cell apoptosis[9,10]. However, since this project did not distinguish between EV subpopulations, the umbrella term extracellular vesicles will be used throughout this report. The use of MSC-derived EVs (MSC-EVs) has been extensively studied as therapy in different CVDs. For instance, multiple studies demonstrated the efficacy of MSC-EVs in reducing cardiac fibrosis and improving cardiac function in mouse models of myocardial ischemia/reperfusion (I/R)[5,11,12]. Similarly, Potz et al. found that MSC-EVs improved cardiac output, increased blood flow, and increased vessel density in swine models of myocardial I/R injury[13]. In regard of immunomodulation, MSC-EVs have been found to reduce the quantity of pro-inflammatory (M1) macrophages, while increasing the number of anti-inflammatory (M2) macrophages in models of dilated cardiomyopathy and myocardial I/R injury[14-16].

Taken together, these findings suggest that MSC-EVs are a viable option to promote cardiac regeneration and treat HF, however, there are still challenges associated with their translation to the clinic. For instance, upscaling EV production is a labor-intensive, time-consuming, and costly process, due to the poor secretion rate of EVs by cells[17,18]. Therefore, various approaches have been tested to increase EV production in cell culture. In this regard, changing the culture conditions and applying or minimizing chemical or physical stressors have been shown to stimulate EV production[19]. For instance, serum starvation is a widely used technique in which cells are initially cultured in serum supplemented media to facilitate cell proliferation, whereupon they are incubated with serum-free (starvation) medium for 24 and 48h prior to EV isolation[20]. In response to serum starvation, cells produce more EVs, while

contaminants, such as endogenous EVs, that are usually present in serum, are minimized[20,21]. However, because serum contains nutrients that are essential for cell survival, it has been demonstrated that serum starvation decreases cell proliferation and affects cell characteristics, hence indirectly influencing the properties of their derived EVs[20-22]. As a result, various research groups examined the effects of supplementation of the starvation medium and were able to increase EV yield, while also maintaining EV quality[23-26]. Nevertheless, despite these efforts, the methodologies remain inadequate for large-scale EV production.

Therefore, numerous chemically defined serum replacements have been developed that facilitate MSC proliferation and not alter cell characteristics, while simultaneously increase EV production on large-scale. For instance, FiberCell Systems' chemically defined medium for high density cell culture (CDM-HD) is believed to increase EV production from MSCs. CDM-HD is a protein-free, animal component-free, and low-particulate serum replacement that is originally developed for high density cell culture and optimized for the use in hollow fiber bioreactors. CDM-HD has been tested in various applications, including for the production of monoclonal antibodies, recombinant proteins, and EVs[27,28]. In all cases, CDM-HD significantly reduced the quantity of contaminants, such as lipids, proteins, and intracellular DNA in the samples while increasing the overall particle yield in the majority of cases. However, it should be taken into account that these vast particle quantities were obtained when paired with FiberCell Systems' hollow fiber bioreactors, which allow cells to grow at 100 times the density of 2D cell culture systems. Solely, FiberCell Systems examined the effect of CDM-HD on EV production in 2D cell culture systems and compared these results with the corresponding starvation medium. These results showed that the basal medium supplemented with 10% CDM-HD increased the concentration of MSC-EVs approximately 8-fold when compared to the starvation medium. Despite the fact that CDM-HD has shown excellent potential for MSC culture and EV upregulation, its effects on MSC viability and morphology, as well as EV protein markers and functionality in 2D cell culture systems, remain ambiguous.

Therefore, this project aimed to assess the effects of culture conditions with CDM-HD on the production of human fetal MSC-EVs (hfMSC-EVs), and whether these EVs are functional. To this end, human fetal MSCs (hfMSCs) were either cultured with starvation media, comprising Opti-MEM or MEM-α, for 24h or with the aforementioned basal media with 10% CDM-HD supplementation for 24 and 48h. Based on EV particle yield and EV protein marker expression, one optimal culture condition was selected and these derived EVs were used in a scratch wound assay to assess functionality.

Material and methods

Cell culture

HfMSCs were cultured in growth medium comprising MEM-α (Gibco, 22561021) supplemented with 10% fetal bovine serum (FBS; Gibco, 10099-141), 1% penicillin/streptomycin (p/s; Gibco, 15140-122), 35.2 µg/mL sodium-L-ascorbic acid (Sigma Aldrich, A4034), and 1 ng/mL basic-fibroblast growth factor (Sigma Aldrich, F0291). Human microvascular epithelial cells-1 (HMECs-1) were cultured in MCDB-131 medium (Gibco, 10372019) supplemented with 10% FBS, 1% p/s, 50 nM hydrocortisone (Sigma Aldrich, H6909), 10 ng/mL human epidermal growth factor (Gibco, PHG6045), and 200 nM L-glutamine (Thermo Scientific, 25030024). When the cells reached a confluency of 85-90%, they were either trypsinized using 0.25% trypsin (Sigma Aldrich, T4049) and passaged to new 0.1% gelatin-coated flasks or plates supplemented with new growth medium, or, in the case of hfMSCs, incubated with the culture condition for EV isolation. All cells were cultured at 37 °C in a 5% CO_2 humidified incubator.

Extracellular Vesicle Production and Isolation

Prior to incubation with the culture condition, hfMSCs were shortly washed with approximately 6 mL phosphate-buffered saline (PBS; Gibco, 10010-015), whereupon the culture condition was added. The culture condition comprised either of basal MEM-α, MEM-α supplemented with 10% CDM-HD (FiberCell Systems) (M+CDM), basal Opti-MEM (Gibco, 31985-070), or Opti-MEM supplemented with 10% CDM-HD (OM+CDM). During the incubation period, the effects of the culture conditions on hfMSC morphology were assessed using an EVOS microscope (Life Technologies). After 24 – 48h of incubation, conditioned media was collected and pooled in 50 mL polypropylene (PP) centrifuge tubes (Sarstedt, 62.547.254) and centrifuged at 350 x g for 5 minutes, to remove floating cells. Next, pellets were discarded and supernatants were further centrifuged at 2,000 x g for 15 minutes, to remove cell debris. The abovementioned centrifugation steps were performed using a 5810R centrifuge (Eppendorf). Afterward, supernatants were filtered through a 0.45 µm filter unit compartment (Thermo Scientific, 166-0045) and divided over 38.5 mL PP ultracentrifuge tubes (Beckman Coulter, 326823), followed by a 70-minute ultracentrifugation (UC) step at 100,000 x g at 4 ºC using an Optima XE-90 Ultracentrifuge (Beckman Coulter), to pellet EVs. Pellets containing EVs were re-suspended in approximately 70 µL PBS and were hereafter referred to as EV samples. Until further analysis, EV samples were stored at 4 ºC. To ensure that the EV samples' purification and processing procedures do not produce artifacts and that functionality can be assigned to hfMSC-derived components rather than components in CDM-HD, procedural controls (PCs) were included and were produced according to the same procedures as the EV samples.

HfMSC Characterization

For protein analysis, hfMSCs were lysed in radioimmunoprecipitation assay (RIPA) lysis buffer (Merck Milipore, 20-188) with protease/phosphatase inhibitors (Cell Signalling Technology, 5872), and centrifuged at 14,000 x g for 10 minutes at 4 °C using a Mikro 220R centrifuge (Hettich). Supernatants were collected, aliquoted, and stored at -80 °C until further analysis. Furthermore, hfMSCs were trypsinized, whereupon cell count and viability were measured using a 0.4% Trypan Blue staining (Sigma Aldrich, T8154) on a TC20 Automated Cell Counter (Bio-RAD). Next, hfMSCs were centrifuged at 350 x g for 5 minutes, whereafter supernatants were discarded and pelleted hfMSCs were dissolved in 200 µL PBS containing 1% bovine serum albumin (BSA; Roche, 10735086001). Next, 100,000 cells per well were collected in a 96-wells U-bottom plate (Greiner Bio-One, 650185) and washed twice with 200 µL PBS/1% BSA and centrifuged at 350 x g for 5 minutes, whereupon supernatants were removed each time. As suggested by the International Society for Cell and Gene Therapy (ISCT), MSCs should express CD73, CD90, and CD105, while lacking CD14 and CD34[29]. Therefore, hfMSCs were directly stained with anti-human CD90-APC (1:50; BD Pharmingen, 555748),

CD73-FITC (1:50; BD Pharmingen, 561254), CD105-FITC (1:50; Bio-Rad, MCA1557), CD14-APC (1:50; Bio-Rad, MCA1568), and CD34-FITC (1:50; ImmunoTools, 21330343) and incubated in the dark for 60 minutes at room temperature (RT). IgG-APC (1:50; BD Pharmingen, 555751) and IgG-FITC (1:50; BD Pharmingen, 555748) were used as isotype controls. After incubation, hfMSCs were washed twice with 200 µL PBS/1% BSA and centrifuged at 350 x g for 5 minutes, to remove unbound antibodies. Finally, hfMSCs were re-suspended in 200 µL PBS/1% BSA and analyzed using a CytoFLEX flow cytometer (Beckman Coulter) with a sample loading speed of 60 µL/min. Acquired data was analyzed with Kaluza software (version 1.5a).

Nanoparticle tracking analysis

Nanoparticle tracking analysis (NTA) was performed to determine the particle concentration and size distribution of the EV samples using a NanoSight NS500 (Malvern Panalytical). EV samples were diluted with PBS in various concentrations to obtain between 30 and 100 particles/frame and vortexed shortly. Per sample four recordings were captured each with a camera set at 16, detection threshold at 5, screen gain at 1, and a 30 second duration. The shutter and gain were manually adjusted for optimal detection and were kept constant throughout experiments. Afterward, recordings were automatically converted into computational data using NanoSight NTA software (version 3.3).

Western blot analysis

Prior to western blot analysis, total protein concentrations of hfMSC cell lysates were determined using a micro bicinchoninic acid (BCA) protein assay (Thermo Scientific, 23235) and measured using a Multiskan FC Microplate Photometer (Thermo Scientific). Afterward, equivalent micrograms of cell lysate' protein and normalized EV sample' volumes were lysed in lithium dodecyl sulphate (LDS) sample buffer (Invitrogen, NP0007) and sample reducing agent (Invitrogen, NP0004). Next, samples were heated for 10 minutes at 95 ºC, loaded on a 4-12% Bis-Tris Plus pre-cast polyacrylamide gel (Invitrogen, NW04125BOX), and ran at 130V for 75 minutes. For dry blotting, migrated samples were transferred at 20V for 7 minutes to a pre-activated polyvinylidene difluoride (PVDF) transfer membrane (Invitrogen, IB24002) using an iBlot 2 transfer device (Life Technologies). Afterward, non-specific binding was blocked by adding 50% (v/v) Intercept Blocking Buffer (LI-COR Biosciences, 927-60001) and Tris-buffered saline (TBS) for approximately 70 minutes at RT, whereupon primary antibodies were added and incubated overnight at 4 ºC. To characterize EVs, mouse anti-CD81 (1:000; Santa Cruz Biotechnology, sc-166029) and mouse anti-syntenin (1:1000; Origene, TA504796) were used, whereas rabbit anti-calnexin (1:1000; GeneTex, GTX101676) was used as an negative control and mouse anti-β-actin (1:1000; Sigma Aldrich, A5441) as a loading control. After incubation, membranes were washed thrice in TBS containing 0.1% Tween-20 (TBS-T; Sigma Aldrich, 8.22184.0500) and incubated with secondary antibodies, Alexa Fluor 680-conjugated anti-mouse antibody (1:7500; LI-COR Biosciences, A-21057) and IRDye 800CW anti-rabbit antibody (1:7500; LI-COR Biosciences, 926–32211), for 50 minutes at RT in the dark. All immune-labelling was performed with 50% (v/v) Intercept Blocking Buffer and TBS-T. To remove unbound antibodies, membranes were washed thrice with TBS-T and TBS for 15 minutes each and analyzed using an Odyssey Infrared Imager (LI-COR Biosciences) at 700 nm and 800 nm.

Scratch wound assay

HMEC-1 cells ($9x10^4$ cells/well; three replicates per group) were seeded into a 48-wells plate (Corning, 3548) and incubated until cells were confluent. On reaching confluency, a sterile p200 pipette tip was used to make a scratch wound across each well, whereupon each well was washed twice with basal MCDB-131 medium, to remove floating cells. Next, HMECs-1 cells were treated with either the EV sample ($2x10^{10}$ particles/well), PC, positive control (20% FBS), or negative control (PBS). All

treatments were dissolved in 200 µL basal MCDB-131 medium per well. The EV sample and PC were normalized based on volume. Wound closure was photographed every hour over the next 24h using an OMNI device (CytoSMART) and analyzed with ImageJ (version 1.47). To calculate the migration distance, the total area and length of each scratch were compared at the start of the experiment (t=0) and after 6h (t=6). The migration distance was then determined by subtracting the value at t=0 from the value at t=6. As a reference, the mean of the negative control wells was used.

Statistics

Statistical analysis was conducted using Graphpad Prism (version 9; GraphPad Software). Graphs are displayed as mean ± standard deviation (SD). Differences were evaluated using an one-way ANOVA and were considered statistically significant at $p < 0.05$.

Results

1. <u>HfMSCs express characterstic MSC surface markers</u>

To date, the expression of specific surface markers has been used to define MSCs. However, various culture conditions have been shown to affect these characteristic surface markers, thereby potentially influencing MSC functionality as well[30]. On that note, it should be taken into consideration that if changes occur in the parental cell, these changes will most likely be translated in their EVs[24]. Therefore, to determine whether the representative MSC surface markers were expressed by the hfMSCs used for the comparative analysis, a MSC characterization utilizing flow cytometry was performed. In accordance to ISCT guidelines, ≥95% of the MSC population should express CD73, CD90, and CD105, whereas they should lack expression (≤2%) of CD14 and CD34[29]. As presented in Fig. 1A, only one peak was produced, independently of the control peak, for the surface markers CD73, CD90, and CD105, suggesting that all cells were positive, albeit weakly, for these markers. On the other hand, surface markers CD14 and CD34 were expressed to the same extent as the isotype control, implying that the cells were negative for these markers. Altogether, these datasets demonstrate that within the test samples, no mixed cell population was found and that the hfMSCs expressed the representative MSC surface markers in accordance to ISCT guidelines.

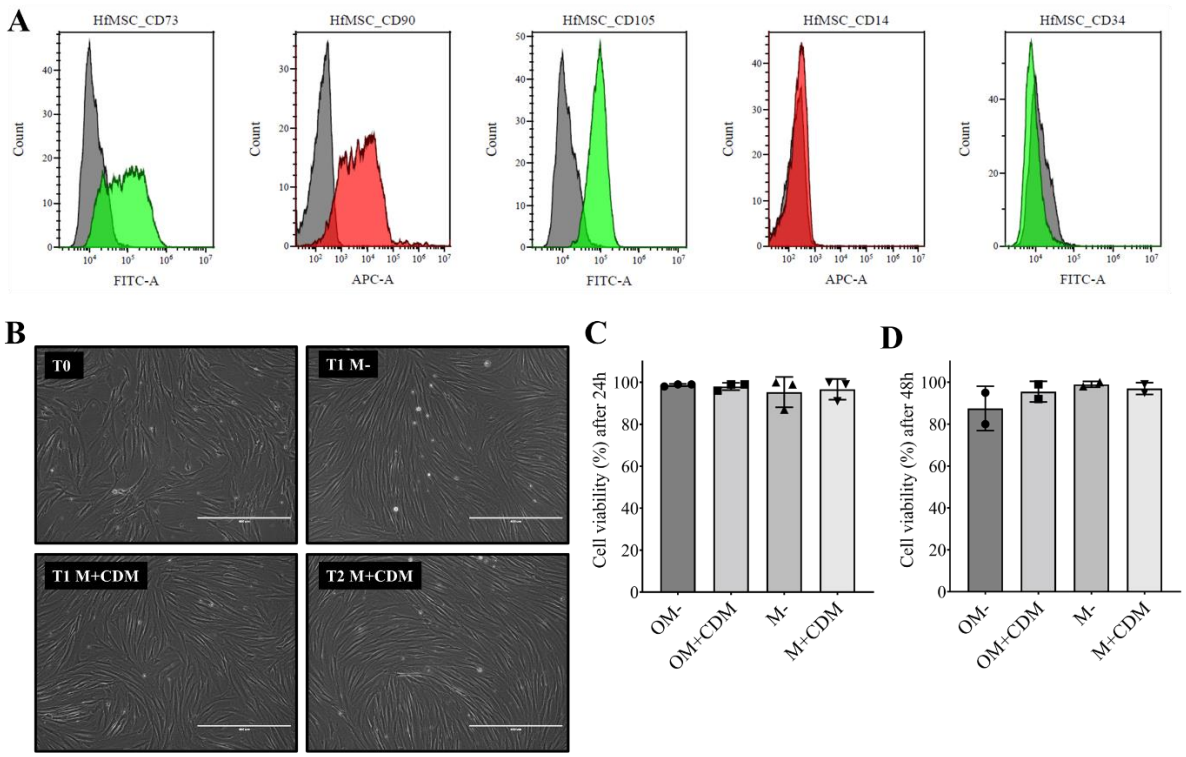

Figure 1. Characterization of cultured hfMSCs. *(A) Surface marker expression patterns of hfMSCs during in vitro culture in MEM+CDM as analyzed by flow cytometry (n=1). HfMSCs were directly stained with fluorochrome-conjugated antibodies against CD73, CD90, CD105, CD14, and CD34. Colored histograms indicate the positive cell populations for each antibody, whereas grey histograms indicate isotype control antibodies. APC=allophycocyanin; FITC=fluorescein isothiocyanate. (B) Images showing hfMSC morphology and proliferation prior to incubation (T0) when cultured in basal MEM-α (M-) for 24 hours (T1) and CDM-HD (M+CDM) over a 48-hour period (T2). Scale bar was set at 400 µm. (C) MSC cell viability measured after 24h. (D) MSC cell viability measured after 48h. The data is presented as the mean of the biological replicates ± standard deviation (C: n=3, D: n=2). No statistical difference was observed between measurements.*

2. CDM-HD maintains hfMSC morphology and cell viability, and facilitates proliferation

Next, the effects of culture with CDM-HD on hfMSC morphology, proliferation, and cell viability were assessed and compared to serum starvation. For this purpose, hfMSCs were cultured in either Opti-MEM or MEM-α, with or without the supplementation of 10% CDM-HD. The impact of CDM-HD on hfMSC morphology, proliferation, and cell viability was assessed after 24 and 48h. In addition, the incubation time with starvation media was limited to 24h to minimize cell apoptosis, as this would otherwise increase the presence of apoptotic bodies in the conditioned medium[20]. As shown in Fig. 1B and Suppl. Fig. 1, the MSCs maintained their uniform fibroblast-like spindle shape for all culture conditions after 24 and 48h. Noteworthily, CDM-HD-cultured hfMSCs became more elongated overtime, which is potentially due to the continued proliferation. Interestingly, despite expectations that proliferation rate would diminish when cells are incubated with starvation media, starved hfMSCs continued to proliferate the following 24h. In regard of cell viability, minor differences were observed after 24 (Fig. 1C) and 48h (Fig. 1D). Collectively, these results indicate that culture with CDM-HD does not impact hfMSC morphology, facilitates proliferation, and preserves cell viability.

3. CDM-HD increases hfMSC-EV yield

Next, to assess whether culture with CDM-HD increases hfMSC-EV production, a comparative analysis was performed wherein the EV yield of CDM-HD-cultured hfMSCs was compared to the hfMSC-EV yield from serum starved hfMSCs. In doing so, hfMSCs were either cultured in starvation media, comprising Opti-MEM or MEM-α, for 24h or with the aforementioned basal media with 10% CDM-HD supplementation for 24 and 48h. Afterward, EV samples were obtained from conditioned media, whereupon their total particle concentrations and particle size distributions were determined using NTA (Fig. 2A, C; 2D, F). To demonstrate that co-isolated CDM-HD does not introduce artifacts in the EV samples, PCs were incorporated for all measurements. As displayed in Suppl. Fig. 2A, NTA results show that the measured particle concentration of the PC is negligible compared to the particle concentration of the M+CDM EV sample. Similarly, protein marker expression for all used protein markers was absent for the PC (Suppl. Fig. 2B). Furthermore, regardless the type of basal media used, CDM-HD-cultured hfMSCs produced greater particle yields than starved hfMSCs over a 24-hour period (Fig. 2A). More specifically, in comparison to the starvation media, culture in OM+CDM resulted in a 9.6-fold increase in particle yield, which was considered statistically significant, while culture in M+CDM increased particle yield with 3.7-fold. When comparing the CDM-HD conditions, culture in OM+CDM resulted in a 1.2-fold greater particle yield than culture in M+CDM.

Furthermore, because CDM-HD was initially intended for continuous harvesting in bioreactor systems, it was hypothesized that a prolonged incubation with CDM-HD would result in greater particle yields. Therefore, incubation with CDM-HD was prolonged to 48h, whereas incubation with the starvation media was maintained at 24h to minimize the occurrence of apoptotic bodies. The results, displayed in Fig. 2D, show that hfMSCs cultured in OM+CDM produced a 9.8-fold greater particle yield than its starvation counterpart, which, interestingly, was not considerably different after 24h. In contrast, when cultured in M+CDM, particle yield was increased 17.2-fold after 48h when compared to the starvation medium. Among CDM-HD conditions, it should be noted that the ratio in yield of OM+CDM and M+CDM shifted, with culture in M+CDM resulting in a greater particle yield (2.3-fold) once incubation was prolonged with 24h. Regarding the particle size distributions among samples, no apparent differences were observed after 24 (Fig. 2C) and 48h (Fig. 2F). Additionally, the detected events above the filter cut-off (>0.45 µm) may be the result of UC-induced particle aggregation[31].

Lastly, in order to characterize and study the differences in protein expression among EV samples, protein content-based EV characterization was performed by western blot analysis. In accordance to the international EV research guidelines, MISEV2018, EV protein characterization was performed by the specific binding of antibodies towards i) a transmembrane protein that is associated to the plasma membrane and/or EVs (CD81), ii) a cytosolic protein recovered in EVs (syntenin), iii) and to a potential non-EV co-isolated structure (calnexin)[32]. As a loading control, anti-β-actin was added. The results, as displayed in Fig. 2B, 2E, confirm that when cultured with CDM-HD higher expressions of EV protein markers, CD81 and syntenin, were detected when compared to the starvation media. Noteworthily, the expression of calnexin was detected within EV samples after 24 and 48h. Collectively, western blot analysis verifies that the particles measured by NTA (Fig. 2A, 2D), consisted of EVs and that the increase in EV yield is a response by the hfMSCs to CDM-HD. Furthermore, because M+CDM resulted in the highest EV yield after 48h, this culture condition was selected to further investigate EV functionality.

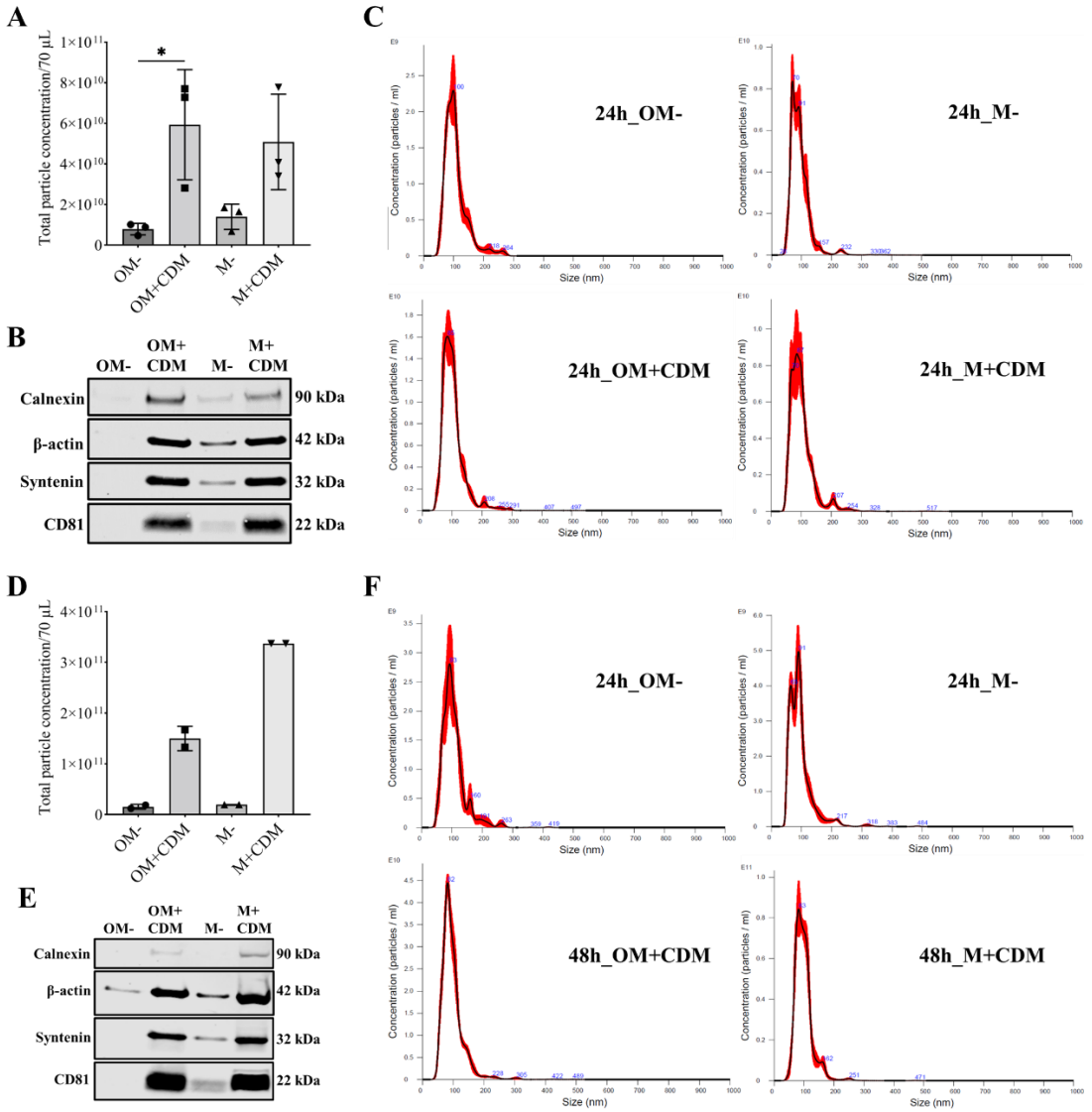

Figure 2. Impact of culture conditions on hfMSC-EV yield and particle size distribution. *HfMSCs were cultured in starvation media, comprising Opti-MEM (OM-) or MEM-α (M-), or with 10% CDM-HD supplementation. Impact on total particle concentration, particle size distribution, and protein expression were evaluated after 24h (A-C) and after 48h (D-F). NTA was performed to assess the total particle concentration (A, D) and particle size distributions (C, F) in the EV samples. The data is presented as the mean of the biological replicates ± standard deviation (A: n=3, D: n=2). Asterisks above the bars denote levels of significance between conditions (*p-value <0.05). (B, E) Western blot analyses showing expression of protein markers calnexin, β-actin, syntenin, and CD81. EV samples were normalized based on volume.*

4. <u>M+CDM EVs induce HMEC-1 migration to a limited extent</u>

Finally, it is generally recognized that EVs stimulate angiogenesis in wound healing, partially through activation of recipient cells via receptor-ligand interactions[8]. Given the importance of cell migration in angiogenesis, the capability of the M+CDM EVs to induce cell migration is crucial for their application in cardiac repair[33]. Therefore, the functionality of M+CDM EVs was assessed in a scratch wound assay. Upon stimulation with the M+CDM EV sample ($2x10^{10}$ particles/well), PC, 20% FBS (positive control) or PBS (negative control), HMEC-1 migration was monitored for the following 6h, whereupon the migration distance was determined and compared to the negative control. The data, displayed in Fig. 3A, shows that the M+CDM EV sample induced HMEC-1 cell migration when compared to the negative control. However, minor differences in migration distance between the M+CDM EV sample and PC were observed during the experiments (Fig. 3B). This hereby suggests that functionality of the M+CDM EV sample is potentially assigned to components isolated along with CDM-HD rather than to the EVs.

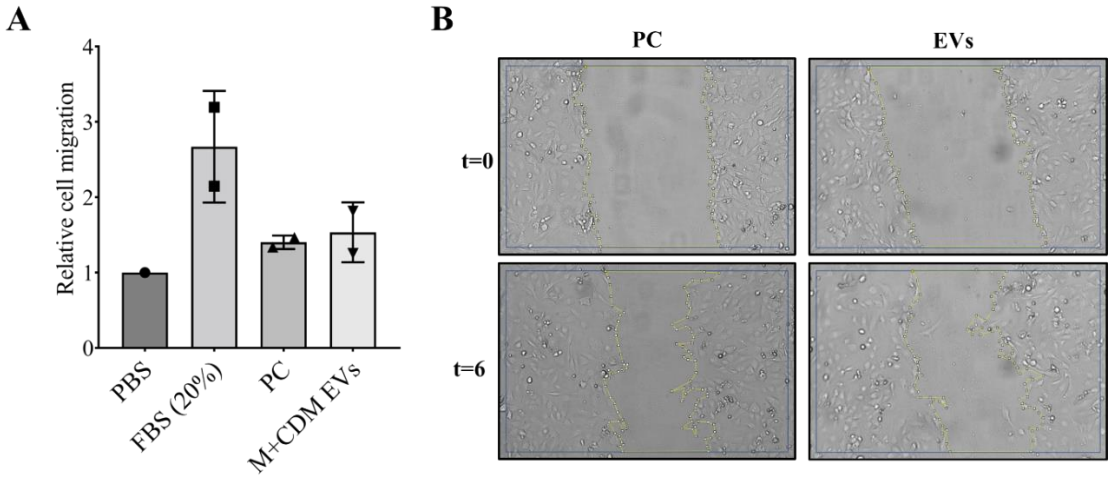

Figure 3. HfMSC-EVs display minor effects in HMEC-1 migration. *(A) The relative migration distance as a measure of wound closure. Each condition was plotted relatively to the negative control (PBS). The data is presented as the mean of the biological replicates ± standard deviation (n=2). (B) Representative images of the HMEC-1 migration when treated with the PC and EV sample shortly after addition of the treatment (t=0) and after 6h (t=6). Scale bar was set at 200 µm.*

Discussion and conclusions

The application of MSC-EVs has been demonstrated to be a promising treatment for cardiac repair. Nevertheless, the exploitation of EVs as therapeutic agents is hampered as upscaling EV production remains cumbersome due to their limited cellular secretion[17,18]. Several attempts have already been made to increase EV yield by combining chemically defined serum replacements, such as CDM-HD, with culture in hollow fiber bioreactors. However, while CDM-HD showed great potential for upscaling EV production, the impact on MSC-EV characteristics and functionality in 2D cell culture systems has not been extensively studied yet. Therefore, this project aimed to assess the effects of culture conditions with CDM-HD on the production of hfMSC-EVs, and whether these EVs are functional.

First, a comparative analysis was performed comparing the yield of hfMSC-EVs from culture with CDM-HD to the hfMSC-EV yield from serum starvation. In doing so, hfMSCs were either cultured with starvation media, comprising Opti-MEM or MEM-α, for 24h or with the aforementioned basal media with 10% CDM-HD supplementation for 24 and 48h. Here, we found that culture with CDM-HD increases EV yield from hfMSCs to a substantial degree, as determined by NTA and western blot, when compared to serum starvation. Interestingly, the data showed that after 24h, OM+CDM increased the particle yield to a greater extent than M+CDM, whereas after 48h, the increase in particle yield of M+CDM was shown to be superior to OM+CDM. Since, no comparative experiments were performed in this study between timepoints when cultured with CDM-HD, and given that this phenomenon has not been previously described in the literature, further testing is required.
Furthermore, NTA and western blot results showed that no procedural artifacts were found during EV sample measurements, verifying that the increase in EV yield is a response by the hfMSCs to CDM-HD. Noteworthily, EV samples from multiple protein analyses (Fig. 2B, 2E) showed contamination with the endoplasmic reticulum marker, calnexin[34]. The abundance in calnexin could be the result of hfMSCs undergoing apoptosis during extended periods of nutrient deprivation. However, the calnexin expression of the CDM-HD EV samples is most likely not due to nutrient deficiency, as CDM-HD was developed to facilitate MSC proliferation as well. Moreover, while serum starvation does in fact act via nutrient deficiency, it should be noted that the likelihood of detecting these vast quantities of calnexin after 24h is not supported by the literature[20,35]. Another explanation could be that the cells were over confluent, due to continuous proliferation by CDM-HD. However, cell viability, as determined by Trypan blue staining, was not particularly affected after any treatment (Fig. 1C-D). Lastly, the possibility remains that cell debris aggregates may have detached from the pellet during EV isolation. However, further testing is needed to support this hypothesis.

Generally, MSC-EVs are known to be capable of stimulating endothelial cell migration by the activation of recipient cells through receptor-ligand interactions[8]. Therefore, to assess the functionality of M+CDM EVs, a scratch wound assay was performed. The results showed that compared to the PC, only minor effects on HMEC-1 migration were observed in response to treatment with the EV sample. As previously suggested, this indicates that the functionality of the EV sample is potentially assigned to the components isolated along with CDM-HD rather than to the EVs. The lack of functionality could have a subset of origins.

First, the added dosage of the EV sample could have been insufficient to activate HMEC-1 migration. In this study, the optimal MSC-EV dosage had not been adequately investigated and the chosen dosage was based on findings in the literature[8]. However, EVs derived from different tissue/cell sources, culture in 2D or 3D systems, and isolation and purification procedures, all affect EV functionality differently and therefore require different EV dosages[36-40]. Therefore, to gain insight into the optimal dosages for the M+CDM EVs, dose-response experiments should be included in future studies.

Second, the isolation method used in this study may had detrimental effects on EV functionality. UC has been widely utilized to isolate EVs from conditioned medium by the separation of particles at high-speed[31]. A study by Mol. et al., compared the effects of UC to size-exclusion chromatography (SEC) on the functionality of cardiomyocyte progenitor cell-derived EVs, reporting that SEC isolation resulted in EVs presenting higher functionality than UC-isolated EVs[40]. This diminished effect on UC-isolated EV functioning was caused by the application of high-speed forces, thereby damaging the signaling molecules on the EV surface and hamper recipient cell activation[40]. Therefore, to acquire a better understanding of the functionality of M+CDM EVs, it is recommended that an EV isolation, such as SEC, is conducted in parallel with UC isolation in future studies.

Third, EV functionality could be compromised by the MSC cell/tissue source. Although expression of the MSC surface markers should comply to the ISCT criteria, the functionality of MSCs from different tissue sources shows variability. For instance, a study conducted by Zhu et al., demonstrated that EVs from pluripotent stem cell-derived MSCs had greater stimulatory effects on chondrocyte migration and proliferation than synovial membrane-derived MSCs[41]. In other studies, AT-derived MSC-EVs exerted higher induction of endothelial cell migration and angiogenesis, in comparison to BM-derived MSC-EVs[42,43]. These findings imply that the absence in functionality observed, in this study, may be cell source-related. Therefore, the functionality of the M+CDM EVs should be further explored in other functionality assays.

Overall, the primary focus of this study was to increase EV production from hfMSCs for large-scale production to realize EV-based therapeutics for HF. However, another bottleneck in the exploitation of cell- and EV-based therapies is the use of sera with undefined compositions, such as FBS, to facilitate cell proliferation[44]. Often these sera introduce contaminants, such as mycoplasma, prions, and viruses, hindering clinical translation, as well as endogenous EVs and other nanoparticles (e.g., protein aggregates), that complicate EV isolation and purification procedures and comparisons among measurements[44]. In this study, it was demonstrated that culture with CDM-HD maintained the proliferation, morphology, and viability of hfMSCs for 48h and was found to not introduce procedural artifacts during EV sample measurements. This indicates that CDM-HD can be a serum replacement for cell expansion purposes, thereby rejecting the use of FBS. However, for 2D cell culture systems, the complete rejection of FBS is unlikely for adherent cells, such as MSCs, since CDM-HD does not contain attachment factors that support cell adhesion after passaging. To overcome this, the use of 3D cell culture systems, such as hollow fiber bioreactors, will minimize the use of FBS since cells do not have to be passaged. Especially when large-scale EV production needs to be achieved, using 3D cell culture systems will significantly increase EV yield, as these systems allow cell culture at high density and continuous EV harvesting[45]. Although a comparative analysis between FBS-cultured and CDM-HD-cultured MSCs is still needed, CDM-HD may be a stepping stone towards cell expansion without FBS, hence standardizing culture conditions and enabling consistent and scalable EV production.

Altogether, in the present study we aimed to explore whether culture with CDM-HD affects the production of hfMSC-EVs, and whether these EVs are functional. Conclusively, our data suggests that culture with CDM-HD enhances hfMSC-EV production to a greater extent than serum starvation. Moreover, the functionality of M+CDM EVs is questionable, as only minor differences in functionality were observed to the PC. Based on our findings, the determination of optimal EV dosage and a better understanding of the impact of isolation methods and cell source on the M+CDM EVs will bring us one step closer to realizing their potential as next-generation therapeutics.

References

1. McDonagh TA, Metra M, Adamo M, et al. 2021 ESC guidelines for the diagnosis and treatment of acute and chronic heart failure. *Eur Heart J.* 2021;42(36):3599-3726. doi: 10.1093/eurheartj/ehab368.

2. Schellenbaum GD, Rea TD, Heckbert SR, et al. Survival associated with two sets of diagnostic criteria for congestive heart failure. *Am J Epidemiol*. 2004;160(7):628-635. doi: 10.1093/aje/kwh268.

3. Guo Y, Yu Y, Hu S, Chen Y, Shen Z. The therapeutic potential of mesenchymal stem cells for cardiovascular diseases. *Cell Death Dis.* 2020;11(5):349-9. doi: 10.1038/s41419-020-2542-9.

4. Hass R, Kasper C, Bohm S, Jacobs R. Different populations and sources of human mesenchymal stem cells (MSC): A comparison of adult and neonatal tissue-derived MSC. *Cell Commun Signal*. 2011;9:12-12. doi: 10.1186/1478-811X-9-12.

5. Lai RC, Arslan F, Lee MM, et al. Exosome secreted by MSC reduces myocardial ischemia/reperfusion injury. *Stem Cell Res.* 2010;4(3):214-222. doi: 10.1016/j.scr.2009.12.003.

6. Joladarashi D, Kishore R. Mesenchymal stromal cell exosomes in cardiac repair. *Curr Cardiol Rep*. 2022;24(4):405-417. doi: 10.1007/s11886-022-01660-1.

7. Banerjee MN, Bolli R, Hare JM. Clinical studies of cell therapy in cardiovascular medicine: Recent developments and future directions. *Circ Res.* 2018;123(2):266-287. doi: 10.1161/CIRCRESAHA.118.311217.

8. Roefs M, Qin J, Bauza-Martinez J, Van De Wakker SI, Vader P, Sluijter J. Cardiac progenitor cell-derived extracellular vesicles promote endothelial cell activation through both associated- and co-isolated proteins. *Cardiovasc Res.* 2022;118(Supplement_1):cvac066.084. https://doi.org/10.1093/cvr/cvac066.084. Accessed 1/24/2023. doi: 10.1093/cvr/cvac066.084.

9. Teng F, Fussenegger M. Shedding light on extracellular vesicle biogenesis and bioengineering. *Adv Sci (Weinh).* 2020;8(1):2003505. doi: 10.1002/advs.202003505.

10. Yanez-Mo M, Siljander PR, Andreu Z, et al. Biological properties of extracellular vesicles and their physiological functions. *J Extracell Vesicles*. 2015;4:27066. doi: 10.3402/jev.v4.27066.

11. Arslan F, Lai RC, Smeets MB, et al. Mesenchymal stem cell-derived exosomes increase ATP levels, decrease oxidative stress and activate PI3K/akt pathway to enhance myocardial viability and prevent adverse remodeling after myocardial ischemia/reperfusion injury. *Stem Cell Res*. 2013;10(3):301-312. doi: 10.1016/j.scr.2013.01.002.

12. Shao L, Zhang Y, Lan B, et al. MiRNA-sequence indicates that mesenchymal stem cells and exosomes have similar mechanism to enhance cardiac repair. *Biomed Res Int*. 2017;2017:4150705. doi: 10.1155/2017/4150705.

13. Potz BA, Scrimgeour LA, Pavlov VI, Sodha NR, Abid MR, Sellke FW. Extracellular vesicle injection improves myocardial function and increases angiogenesis in a swine model of chronic

ischemia. *J Am Heart Assoc*. 2018;7(12):e008344. doi: 10.1161/JAHA.117.008344. doi: 10.1161/JAHA.117.008344.

14. Sun X, Shan A, Wei Z, Xu B. Intravenous mesenchymal stem cell-derived exosomes ameliorate myocardial inflammation in the dilated cardiomyopathy. *Biochem Biophys Res Commun*. 2018;503(4):2611-2618. doi: 10.1016/j.bbrc.2018.08.012.

15. Shen D, He Z. Mesenchymal stem cell-derived exosomes regulate the polarization and inflammatory response of macrophages via miR-21-5p to promote repair after myocardial reperfusion injury. *Ann Transl Med*. 2021;9(16):1323-3557. doi: 10.21037/atm-21-3557.

16. Zhao J, Li X, Hu J, et al. Mesenchymal stromal cell-derived exosomes attenuate myocardial ischaemia-reperfusion injury through miR-182-regulated macrophage polarization. *Cardiovasc Res*. 2019;115(7):1205-1216. doi: 10.1093/cvr/cvz040.

17. Goh WJ, Zou S, Ong WY, et al. Bioinspired cell-derived nanovesicles versus exosomes as drug delivery systems: A cost-effective alternative. *Sci Rep*. 2017;7(1):14322-x. doi: 10.1038/s41598-017-14725-x.

18. Watson DC, Bayik D, Srivatsan A, et al. Efficient production and enhanced tumor delivery of engineered extracellular vesicles. *Biomaterials*. 2016;105:195-205. doi: 10.1016/j.biomaterials.2016.07.003.

19. Hahm J, Kim J, Park J. Strategies to enhance extracellular vesicle production. *Tissue Eng Regen Med*. 2021;18(4):513-524. doi: 10.1007/s13770-021-00364-x.

20. Li J, Lee Y, Johansson HJ, et al. Serum-free culture alters the quantity and protein composition of neuroblastoma-derived extracellular vesicles. *J Extracell Vesicles*. 2015;4:26883. doi: 10.3402/jev.v4.26883.

21. Shelke GV, Lasser C, Gho YS, Lotvall J. Importance of exosome depletion protocols to eliminate functional and RNA-containing extracellular vesicles from fetal bovine serum. *J Extracell Vesicles*. 2014;3:10.3402/jev.v3.24783. eCollection 2014. doi: 10.3402/jev.v3.24783.

22. Sluijter JPG, Davidson SM, Boulanger CM, et al. Extracellular vesicles in diagnostics and therapy of the ischaemic heart: Position paper from the working group on cellular biology of the heart of the european society of cardiology. *Cardiovasc Res*. 2018;114(1):19-34. doi: 10.1093/cvr/cvx211.

23. Lopatina T, Bruno S, Tetta C, Kalinina N, Porta M, Camussi G. Platelet-derived growth factor regulates the secretion of extracellular vesicles by adipose mesenchymal stem cells and enhances their angiogenic potential. *Cell Commun Signal*. 2014;12:26-26. doi: 10.1186/1478-811X-12-26.

24. de Jong OG, Verhaar MC, Chen Y, et al. Cellular stress conditions are reflected in the protein and RNA content of endothelial cell-derived exosomes. *J Extracell Vesicles*. 2012;1:10.3402/jev.v1i0.18396. eCollection 2012. doi: 10.3402/jev.v1i0.18396.

25. King HW, Michael MZ, Gleadle JM. Hypoxic enhancement of exosome release by breast cancer cells. *BMC Cancer*. 2012;12:421-421. doi: 10.1186/1471-2407-12-421.

26. Scheiber AL, Clark CA, Kaito T, et al. Culture condition of bone marrow stromal cells affects quantity and quality of the extracellular vesicles. *Int J Mol Sci*. 2022;23(3):1017. doi: 10.3390/ijms23031017. doi: 10.3390/ijms23031017.

27. Moya-Torres A, Gupta M, Heide F, et al. Homogenous overexpression of the extracellular matrix protein netrin-1 in a hollow fiber bioreactor. *Appl Microbiol Biotechnol*. 2021;105(14-15):6047-6057. doi: 10.1007/s00253-021-11438-0.

28. Saludas L, Garbayo E, Ruiz-Villalba A, et al. Isolation methods of large and small extracellular vesicles derived from cardiovascular progenitors: A comparative study. *Eur J Pharm Biopharm*. 2022;170:187-196. doi: 10.1016/j.ejpb.2021.12.012.

29. Dominici M, Le Blanc K, Mueller I, et al. Minimal criteria for defining multipotent mesenchymal stromal cells. the international society for cellular therapy position statement. *Cytotherapy*. 2006;8(4):315-317. doi: 10.1080/14653240600855905.

30. Sotiropoulou PA, Perez SA, Salagianni M, Baxevanis CN, Papamichail M. Characterization of the optimal culture conditions for clinical scale production of human mesenchymal stem cells. *Stem Cells*. 2006;24(2):462-471. doi: 10.1634/stemcells.2004-0331.

31. Linares R, Tan S, Gounou C, Arraud N, Brisson AR. High-speed centrifugation induces aggregation of extracellular vesicles. *J Extracell Vesicles*. 2015;4:29509. doi: 10.3402/jev.v4.29509.

32. Thery C, Witwer KW, Aikawa E, et al. Minimal information for studies of extracellular vesicles 2018 (MISEV2018): A position statement of the international society for extracellular vesicles and update of the MISEV2014 guidelines. *J Extracell Vesicles*. 2018;7(1):1535750. doi: 10.1080/20013078.2018.1535750.

33. Lamalice L, Le Boeuf F, Huot J. Endothelial cell migration during angiogenesis. *Circ Res*. 2007;100(6):782-794. doi: 10.1161/01.RES.0000259593.07661.1e.

34. Lasser C, Eldh M, Lotvall J. Isolation and characterization of RNA-containing exosomes. *J Vis Exp*. 2012;(59):e3037. doi(59):e3037. doi: 10.3791/3037.

35. Haraszti RA, Miller R, Dubuke ML, et al. Serum deprivation of mesenchymal stem cells improves exosome activity and alters lipid and protein composition. *iScience*. 2019;16:230-241. doi: 10.1016/j.isci.2019.05.029.

36. Baglio SR, Rooijers K, Koppers-Lalic D, et al. Human bone marrow- and adipose-mesenchymal stem cells secrete exosomes enriched in distinctive miRNA and tRNA species. *Stem Cell Res Ther*. 2015;6(1):127-z. doi: 10.1186/s13287-015-0116-z.

37. Shekari F, Nazari A, Assar Kashani S, Hajizadeh-Saffar E, Lim R, Baharvand H. Pre-clinical investigation of mesenchymal stromal cell-derived extracellular vesicles: A systematic review. *Cytotherapy*. 2021;23(4):277-284. doi: 10.1016/j.jcyt.2020.12.009.

38. Cao J, Wang B, Tang T, et al. Three-dimensional culture of MSCs produces exosomes with improved yield and enhanced therapeutic efficacy for cisplatin-induced acute kidney injury. *Stem Cell Res Ther*. 2020;11(1):206-2. doi: 10.1186/s13287-020-01719-2.

39. Monguio-Tortajada M, Galvez-Monton C, Bayes-Genis A, Roura S, Borras FE. Extracellular vesicle isolation methods: Rising impact of size-exclusion chromatography. *Cell Mol Life Sci*. 2019;76(12):2369-2382. doi: 10.1007/s00018-019-03071-y.

40. Mol EA, Goumans M, Doevendans PA, Sluijter JPG, Vader P. Higher functionality of extracellular vesicles isolated using size-exclusion chromatography compared to ultracentrifugation. *Nanomedicine*. 2017;13(6):2061-2065. doi: 10.1016/j.nano.2017.03.011.

41. Zhu Y, Wang Y, Zhao B, et al. Comparison of exosomes secreted by induced pluripotent stem cell-derived mesenchymal stem cells and synovial membrane-derived mesenchymal stem cells for the treatment of osteoarthritis. *Stem Cell Res Ther*. 2017;8(1):64-9. doi: 10.1186/s13287-017-0510-9.

42. Pomatto M, Gai C, Negro F, et al. Differential therapeutic effect of extracellular vesicles derived by bone marrow and adipose mesenchymal stem cells on wound healing of diabetic ulcers and correlation to their cargoes. *Int J Mol Sci*. 2021;22(8):3851. doi: 10.3390/ijms22083851. doi: 10.3390/ijms22083851.

43. Chance TC, Herzig MC, Christy BA, et al. Human mesenchymal stromal cell source and culture conditions influence extracellular vesicle angiogenic and metabolic effects on human endothelial cells in vitro. *J Trauma Acute Care Surg*. 2020;89(2S Suppl 2):S100-S108. doi: 10.1097/TA.0000000000002661.

44. Lehrich BM, Fiandaca MS. Foetal bovine serum influence on in vitro extracellular vesicle analyses. *J Extracell Vesicles*. 2021;10(3):e12061. doi: 10.1002/jev2.12061.

45. Gobin J, Muradia G, Mehic J, et al. Hollow-fiber bioreactor production of extracellular vesicles from human bone marrow mesenchymal stromal cells yields nanovesicles that mirrors the immuno-modulatory antigenic signature of the producer cell. *Stem Cell Res Ther*. 2021;12(1):127-3. doi: 10.1186/s13287-021-02190-3.

Supplementary results

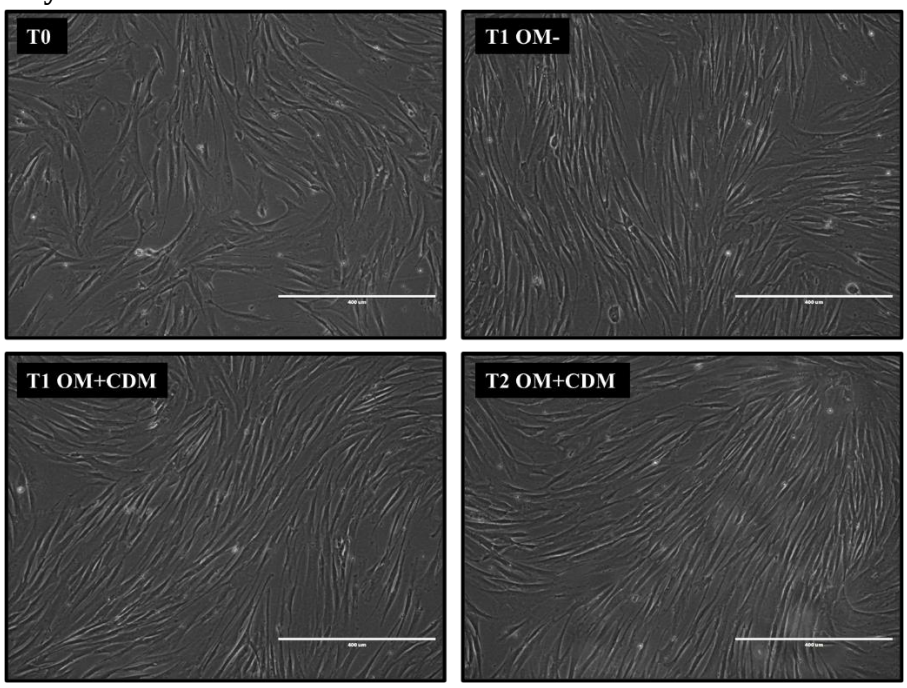

Supplementary Figure 1. Characterization of cultured hfMSCs. *Images showing hfMSC morphology and proliferation prior to incubation (T0) when cultured in basal Opti-MEM (OM-) for 24 hours (T1) and CDM-HD (OM+CDM) over a 48-hour period (T2). Scale bar was set at 400 µm.*

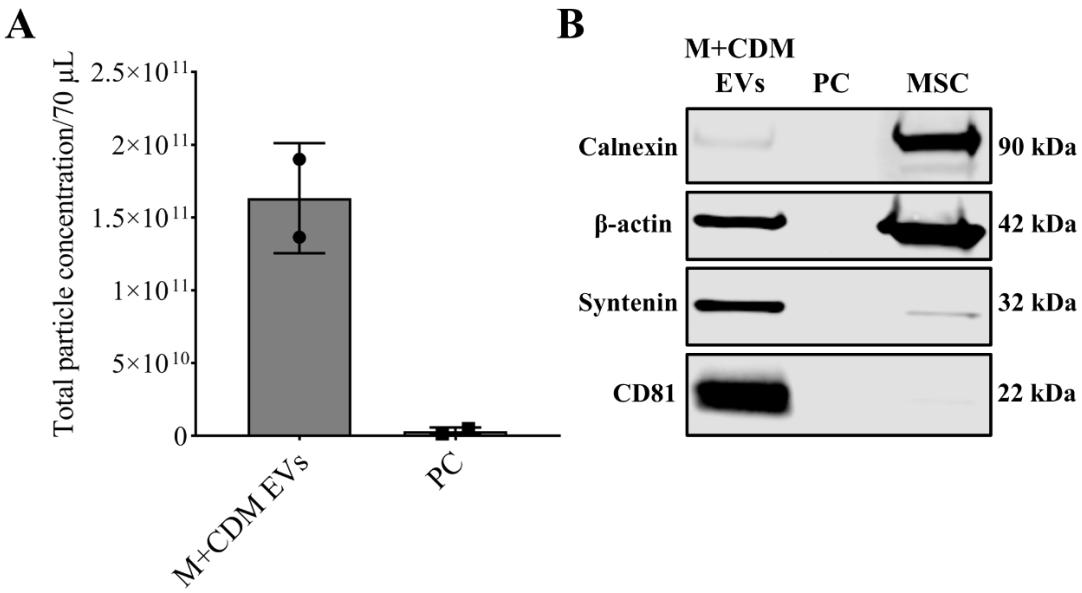

Supplementary Figure 2. Procedural artifacts in NTA and western blot analyses. *(A) Comparison of total particle concentration of a M+CDM EV sample vs. a MEM-α PC. The data is presented as the mean of the biological replicates ± standard deviation (n=2). (B) Western blot analysis showing the expression of protein markers calnexin, β-actin, syntenin, and CD81 for the M+CDM EV sample, whereas none of these were expressed for the PC. MSC cell lysate was indicated as MSC. Results show that no procedural artifacts were identified during the procedures and measurements of the EV sample.*